An elastic second skin

Betty Yu¹, Soo-Young Kang¹, Ariya Akthakul², Nithin Ramadurai², Morgan Pilkenton¹, Alpesh Patel¹, Amir Nashat², Daniel G. Anderson^{3,4,5,6}, Fernanda H. Sakamoto^{7,8}, Barbara A. Gilchrest⁸, R. Rox Anderson^{4,7,8} and Robert Langer^{3,4,5,6}*

We report the synthesis and application of an elastic, wearable crosslinked polymer layer (XPL) that mimics the properties of normal, youthful skin. XPL is made of a tunable polysiloxane-based material that can be engineered with specific elasticity, contractility, adhesion, tensile strength and occlusivity. XPL can be topically applied, rapidly curing at the skin interface without the need for heat- or light-mediated activation. In a pilot human study, we examined the performance of a prototype XPL that has a tensile modulus matching normal skin responses at low strain (<40%), and that withstands elongations exceeding 250%, elastically recoiling with minimal strain-energy loss on repeated deformation. The application of XPL to the herniated lower eyelid fat pads of 12 subjects resulted in an average 2-grade decrease in herniation appearance in a 5-point severity scale. The XPL platform may offer advanced solutions to compromised skin barrier function, pharmaceutical delivery and wound dressings.

he skin is a versatile organ with multiple physiological functions, performed in the context of a fluctuating environment. Importantly, the skin is a visible organ and, thus, makes a psychosocial statement about the health of the individual. The primary function of skin is to provide a protective barrier that mitigates exposure to external factors such as extreme temperatures, toxins, microorganisms, radiation, and mechanical insult, while maintaining the internal milieu.

The important role of skin is inevitably compromised by ageing, environmental insult, and certain disease states. Conditions characterized by skin barrier dysfunction remain prevalent in the population^{1–4}. Cutaneous water loss is clinically observed as chronic inflammation and pruritus that are, in turn, responsible for decreased quality of life, deranged sleep patterns, and mood disturbances that include anxiety and depression⁵. Skin ageing, whether chronological or accelerated by sun exposure, creates persistent problems that will be faced by all members of society⁶. As the skin ages, it loses biomechanical integrity, while also becoming more susceptible to environmental injury⁶ and impaired wound healing⁷.

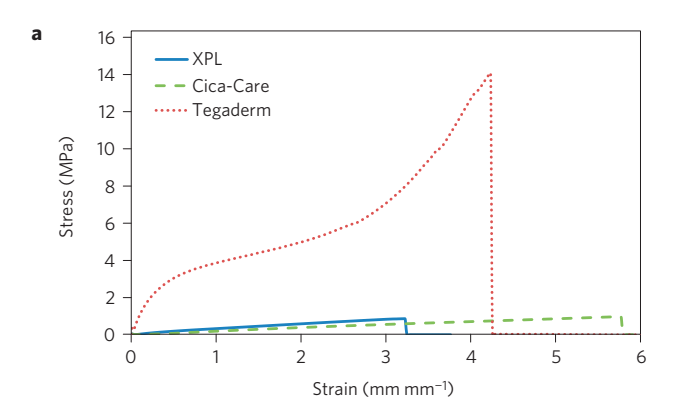
The ageing-related changes in skin mechanical integrity result primarily in loss of elastic recoil and baseline laxity. This loss of elastic recoil is not reversible by existing therapies⁸ and consequently remains the universal fate of our largest and most visible organ⁹. Recent progress in materials science and engineering has yielded flexible skin interfacing technologies^{10–12} that are functionalized in some cases for pharmaceutical delivery¹³, rapid analyte detection¹⁴, continuous physiological monitoring of medical conditions¹⁵, and wound healing^{16–18}. Unfortunately, these advances have not focused on restoring the mechanical and aesthetic properties of the skin to match its original, youthful state.

Existing solutions fall short of addressing both the mechanical and physiological functions of normal healthy skin. Individuals with compromised skin barrier function, for example, still rely on the use of cumbersome occlusive dressings, often in combination with topical ointments that often fail owing to poor patient compliance³. Although existing flexible and skin-adherent pre-formed films interface with the skin^{15,19-21}, these materials are not designed to serve as a 'second skin' that can be worn invisibly to restore normal skin recoil and aesthetics.

The design and adoption of such a 'second skin' with respect to a wearable, skin-conformal material that is topically applied pose several fundamental challenges. First, the material must be safe on skin without irritation and sensitization. Second, the material must be incorporated in a topical formulation that is readily spreadable on skin and form a safe 'second skin' *in situ*. Third, the material must adhere to skin, while providing a breathable, but protective, interface to the environment. Fourth, the material must possess mechanical properties that accommodate normal skin mechanical responses to motion while reinforcing inherent skin tension and elastic recoil. Fifth, the material must mimic, or at least not interfere with, the appearance of healthy normal skin, for a wide range of individual skin types.

On the basis of the above design challenges, we selected the XPL chemistry for siloxane polymers and their associated crosslinked networks in part as a result of the numerous safety and biocompatibility data existing in the literature^{22,23}. In addition to the established safety profile, silicone crosslinked networks offer readily tunable architectures that enable the development of materials that are optimizable for a myriad target mechanical and transport properties, such as flexibility, elongation, elasticity, toughness, adhesion and moisture/oxygen permeability. The

¹Living Proof, Inc., Cambridge, Massachusetts 02142, USA. ²Olivo Laboratories, LLC, Cambridge, Massachusetts 02142, USA. ³Institute for Medical Engineering and Science, Massachusetts Institute of Technology, Cambridge, Massachusetts 02139, USA. ⁴Harvard-MIT Division of Health Science and Technology, Massachusetts Institute of Technology, Cambridge, Massachusetts 02139, USA. ⁵David H. Koch Institute for Integrative Cancer Research, Massachusetts Institute of Technology, Cambridge, Massachusetts 02139, USA. ⁶Department of Chemical Engineering, Massachusetts Institute of Technology, Cambridge, Massachusetts 02139, USA. ⁷The Wellman Center for Photomedicine, Massachusetts General Hospital and Harvard Medical School, Boston, Massachusetts 02114, USA. ⁸Department of Dermatology, Massachusetts General Hospital and Harvard Medical School, Boston, Massachusetts 02114, USA. *e-mail: rlanger@mit.edu



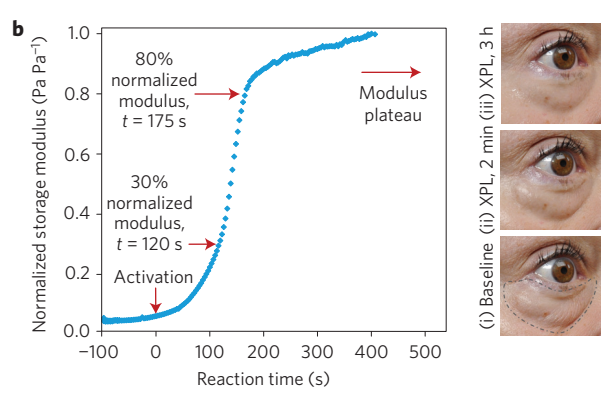


Figure 1 | Mechanical properties of XPL and its crosslinking kinetics. a, Representative tensile stress-strain plots for XPL and two commercial pre-formed wound dressings: Cica-Care silicone sheets and Tegaderm polyurethane sheets with acrylic adhesive backing. Topically applied XPL and pre-formed Cica-Care silicone sheets exhibit good elastic recoil until break. In contrast, pre-formed Tegaderm polyurethane sheets exhibit plastic deformation profiles that yield after 15% strain. **b**, XPL crosslinking kinetics. Crosslinking kinetics of the topical Step 1 formulation containing active prepolymers are represented by the normalized XPL storage modulus as a function of reaction time. The S-shape curve was obtained using the rheometer test for crosslinking kinetics (see Methods). Moduli are normalized by the storage modulus measured at the last time point. In the method, three distinct regions of the reaction are observed with respect to the rate of increase in storage modulus (the slope of the reaction curve). The first region captures the catalyst-stabilizer effect, where the reaction is suppressed by chemically stabilizing the platinum catalyst to allow sufficient sample preparation time before the rheometer records the beginning of the actual cure kinetics. The steep increase in the storage modulus after 100 s signals the rapid crosslinking from hydrosilylation over the next 100 s. After 200 s, the storage modulus increases asymptotically as the crosslinking reaction approaches completion. Photographs illustrating the impact of modulus build on compressing the herniated fat pad are shown. (i) Prominent fat pad protrusion (lower lid bag severity grade 4 is defined by the concavity at the lower tear trough at baseline). XPL was applied to the region demarcated by the dashed line. (ii) Two minutes following XPL application, the skin texture was smoother and the skin laxity seen by the mild skin wrinkling at the medial and central fat pads was tightened. (iii) At 3 h following XPL application, the peak compression

room-temperature, platinum-catalysed hydrosilylation chemistry we selected does not yield reaction by-products that are typical of condensation reactions, nor is it dependent on additional energy sources, such as heat or ultraviolet, required to initiate the topical crosslinking reaction *in situ*. Therefore, the XPL can be safely and easily deposited on skin *in situ* using a two-step topical delivery system, where the first step comprises the application of a flowable, skin-conformal, reactive polysiloxane component that is then crosslinked on exposure to the platinum catalyst that is introduced in the second step. The two-step system also enables optical modulation of the second skin by depositing light scattering particles at the XPL surface from the second step delivery vehicle. The complement of the surface optical particles and the underlying crosslinked polysiloxane network generates a specular and diffuse reflectance approximating the appearance of youthful skin.

In essence, the XPL presented in this study is a skin-adherent, three-dimensional (3D) polymer network that is chemically crosslinked *in situ* on skin, following a two-step topical application process. Each of the materials selected in the formulations is either on the US Food and Drug Administrations list of Generally Regarded as Safe substances, or has individual safety documents that demonstrate safety for leave-on skin applications. Here, we report the design and development of a biomimetic skin-conforming crosslinked polymer material that can be formulated for easy topical application to form an 'invisible' elastic film *in situ*. The film can be safely worn on the skin, restores normal skin aesthetics, and exerts stresses in the plane of the skin to change its form. The tunability of the XPL chemistry and its corresponding ingredients in the topical formulation render this 'second skin' platform potentially useful for a wide range of cosmetic and medical applications.

Results

The development of a wearable 'second skin' began with the design and optimization of XPL materials to mimic the mechanical properties of natural skin, with respect to elastic recoil, flexibility and elongation, to achieve optimal skin-conformal performance.

Synthesis of network architecture that optimizes elastic response.

Uniaxial tensile testing that investigated skin anisotropy with respect to the Langer lines (topological lines corresponding to structural orientation of collagen fibres in the dermis) at different body locations and orientations reported a linear elastic deformation zone at low strains (up to 10–40%) and corresponding elastic moduli ranging from 0.5 to 1.95 MPa, with the resulting fracture strain measured at 140–180%²⁴. On the basis of these established skin mechanical properties, the target XPL modulus space was identified at 0.5 to 1.95 MPa, and the elastic strain region was specified to be greater than 180%.

To identify polymer compositions exhibiting the target design criteria, a material library was generated by systematically varying the following parameters: relative functional (vinyl- and hydride-) polysiloxane chain lengths; the crosslink density as a function of the corresponding functional polysiloxane concentrations; and the concentration of reinforcing fumed silica. A plot of the fracture strain as a function of the tensile modulus illustrates the mechanical design space spanned by the materials synthesized from the screen (see Supplementary Fig. 7), where more than 100 reactive polymer blend (RPB) compositions yielded tensile moduli ranging from 0.1 to 2.5 MPa and fracture strains as high as 800%. On the basis of an analysis of reported values, we restricted our analysis of the library to formulations with tensile moduli between 0.4 and 0.8 MPa. A lead RPB candidate, with tensile modulus of 0.48 MPa, fracture strain of 826%, and adhesive strength of 78 N mm⁻¹, that also satisfied the elasticity criteria (plastic strain of 1.3% and hysteresis strain-energy density loss of 0.66 kJ m⁻³ following cyclic loading at 15% strain) was selected on the basis of an optimization of the material performance attributes desired for a biomimetic 'second skin' (see Supplementary Table 1). This lead RPB was later incorporated with other excipients into the final two-step delivery system to form the XPL in situ.

Although the fumed silica imparts mechanical toughness to the XPL films, it also exponentially increased the viscosity of the RPB. As a result, the lead RPB (containing 27% w/w fumed silica) demonstrated poor topical spreading properties, with a viscosity of



Figure 2 | The visual impact of a 2-grade improvement (from grade 3 to grade 1) after applying XPL to the under-eye area. This image is an illustrative example of a 2-grade improvement, which was consistently observed following repeated split-face application of XPL (*n* > 10).

 $600 \, \mathrm{Pa} \, \mathrm{s}^{-1}$ ($600,000 \, \mathrm{cP}$) measured at $0.5 \, \mathrm{s}^{-1}$. At such a high viscosity, the RPB spreadability on skin approximated that of highly viscous resins such as tar pitch. The detailed formulation strategies of this material are discussed in the Methods.

Mechanical properties of the XPL. Three key mechanical design criteria in the development of the skin mimetic XPL required that the elastic recoil, flexibility and elongation approximated the values of natural skin subjected to an initial elastic large deformation zone (strain under 40% and tensile modulus of 0.5-1.95 MPa)^{25,26}. In Fig. 1a, we report that the XPL maintained elastic recoil until break (fracture strain: $250 \pm 82\%$) and the tensile modulus $(0.51 \pm 0.01 \text{ MPa})$ measured was comparable to that of natural skin. The measure of elastic recoil (elasticity) was based on the energy loss during the load-unload cycles of the material, quantifiable from the area under the hysteresis loop of the stress-strain profile during tensile testing (hysteresis strain-energy density loss). The measured XPL elasticity was 16.8 ± 0.8 kJ m⁻³ of hysteresis strainenergy density loss, following 25 load–unload cycles at 100% strain. We tested elasticity at 100% strain to capture a conservative safety factor of material performance that stretches beyond the reported elastic region for normal skin (less than 40% strain).

With the above mechanical properties to match those of natural skin, we compared the XPL as a wearable skin-conforming material with example commercial benchmarks of film wear on skin, either through pre-formed wound dressings or topical film former formulations.

First, the XPL was compared with two commercial benchmarks of pre-formed wound dressings: Cica-Care silicone gel sheets (Smith and Nephew) and Tegaderm polyurethane sheets coated with acrylic adhesive (3M). As shown in Fig. 1a, similar to the XPL, preformed Cica-Care silicone elastomer sheets exhibited robust elastic recoil until break (fracture strain: $553 \pm 82\%$), with an order of magnitude lower tensile modulus (0.08 ± 0.04 MPa) compared with that of natural skin (0.5–1.95 MPa). These results confirmed that the topically deposited XPL provides a 3D silicone network comparable to pre-formed commercial silicone elastomer sheets, with mechanical properties much closer to those of natural skin.

In contrast to the Cica-Care, pre-formed Tegaderm polyurethane sheets exhibited plastic deformation profiles that yield after 15% strain, highlighting an elastic strain region much less than that of natural skin. Moreover, the measured Tegaderm tensile modulus of 8.85 ± 2.20 MPa was approximately 7 times greater than natural skin. For comparison, Tegaderm exhibited substantially greater plastic deformation than XPL following 25 load–unload cycles at 100% strain, as seen by the order of magnitude increases in the hysteresis strain-energy density loss and plastic strain measured at $237.0\pm25.5\,\mathrm{kJ}\,\mathrm{m}^{-3}$ and $13.56\pm1.25\%$, respectively.

Poor elasticity was also measured for the film deposited from the topical film-forming waterborne polyurethane dispersion Avalure UR 450 polymer (Lubrizol), a raw material ingredient used in topical

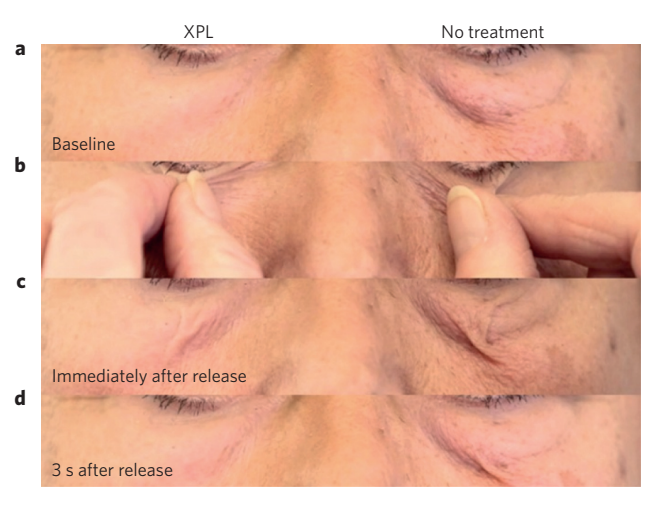


Figure 3 | Time-lapse photos extracted from video footage of skin retraction following a dermatological tenting test. XPL was applied to the right side. The left side served as the untreated control. **a-d**, The four frames extracted show the left and the right side before tenting (**a**), during the tenting test (gentle pinch) (**b**), immediately after the skin is released (**c**), and 3 s after the skin is released (**d**). The side wearing the XPL demonstrates minimal plastic strain and retracts to the original position, whereas the untreated side demonstrates poor elastic recoil and sustained the plastic strain resulting from the imposed stress. These results were consistent with repeated tenting studies (*n* > 10).

personal care products such as make-up, sunscreens and barrier creams. Polyurethane film cast from Avalure UR 450 polymer demonstrated a tensile modulus that was greater than 30 times that of natural skin (37.6 MPa) and that yielded after 15% strain. Supplementary Fig. 9 compares the stress–strain hysteresis loops for polyurethane film cast from Avalure UR 450 polymer and the XPL, where polyurethane Avalure UR 450 yielded with a 12% loss in tensile modulus and plastically deformed with 2% plastic strain, after only 15 load–unload cycles at 15% strain.

In light of the mechanical characteristics exhibited by the commercial benchmarks, these results further reinforced the uniqueness of the XPL composition as a topically applied, skin-adherent, elastomeric network with mechanical properties optimized to match those of natural skin in motion. Moreover, the XPL demonstrated superior skin cosmesis when compared with the commercial benchmarks. Pre-formed Cica-Care silicone sheets are 20 times thicker (1,300 μm) and visibly prominent on the skin, resulting from the glossy, light reflective optics that also delineate the film boundary. The 40- μm -thick films (Tegaderm and polyurethane film cast from Avalure UR 450 polymer), which approximated the XPL thickness, were also highly visible on skin as a result of the mismatched film optics, which were further accentuated by the generation of film wrinkling patterns on skin in motion.

In vivo application and use. This section describes four *in vivo* studies evaluating the XPL utility as a natural-looking, elastic 'second skin'. Pilot human studies were performed to measure changes in the skin mechanical properties and barrier function after wearing XPL on the lower lids where under-eye fat pads may be prominent (Study A) and on normal volar forearm skin (Study B). To further investigate the XPL as a 'second skin' for conditions of compromised barrier function, transepidermal water loss (TEWL) was measured in clinically dry leg skin (Study C). Finally, the clinical performance of the XPL was evaluated in a double-blind, randomized, placebocontrolled study to demonstrate the translation of the above design criteria (safe, topically formed *in situ*, skin-adherent, skinconforming barrier protection, and natural-looking) to the skin of the lower lid application sites during normal wear (Study D).

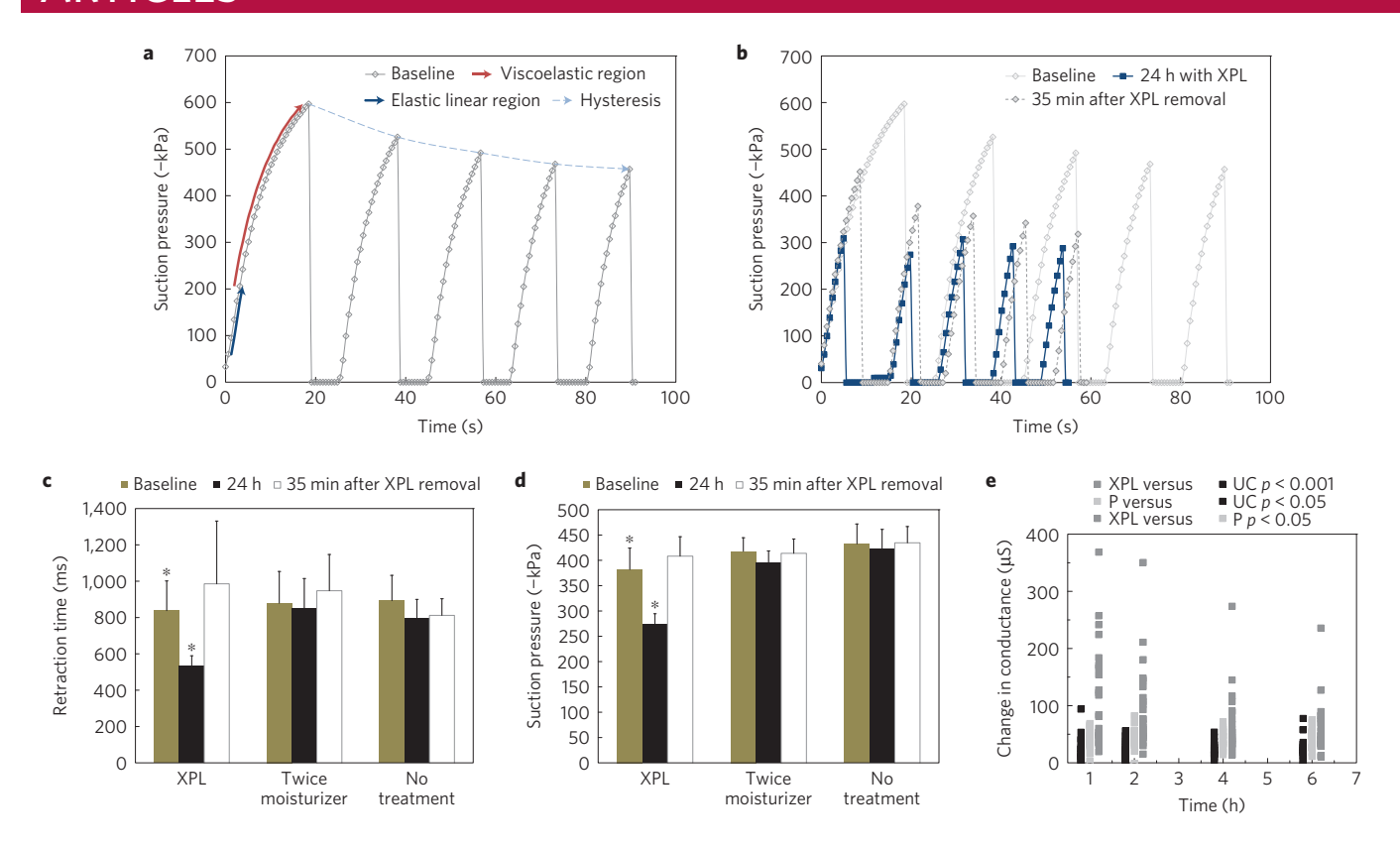


Figure 4 | Pilot study evaluating XPL-induced changes in skin elasticity (Study B) when worn over 24 h on normal volar forearm skin. a, At baseline, a representative plot of the negative pressure required to extend the skin to a fixed height using the suction cup method is shown. The two distinct regions highlighted in red and blue correspond to the viscoelastic and the elastic skin response regions, respectively. The hysteresis experienced following each skin distension cycle is shown by the dashed blue line. b, Following 24 h of XPL wear, the treated skin sites demonstrated increased elastic behaviour, showing a linear elongation response with time (blue squares) for the same representative skin sites. Thirty-five minutes following XPL removal, after 24 h of wear (filled diamonds), the skin approached the baseline behaviour. c, The average skin retraction time was measured for six different individuals. The three treatments were applied to each arm, yielding duplicate treatment sites assigned using a predetermined rotational scheme for each subject. The sites exposed to XPL demonstrated a marked decrease in the skin retraction time (from $838\pm164\,\mathrm{ms}$ to $533\pm57\,\mathrm{ms}$, p<0.005, paired Student's t-test) compared with the baseline values, unlike the 12% lactic acid moisturizer applied twice, initially and after 12 h (879 ± 174 ms to 851 ± 164 ms, not significant (NS)) and the untreated control sites (893±140 ms to 795±104 ms, NS). Thirty-five minutes after XPL removal, the skin recoil time and the corresponding elongation pressures returned to the baseline values. The negative pressure recorded at 12% distension similarly decreased 29% (from 382 ± 42 kPa to 273 ± 22 kPa). **d**, In the same six subjects, p < 0.05 compared with the baseline values, unlike the twice-treated moisturizer sites (418 ± 27 kPa to 396 ± 23 s, NS) and the untreated control sites (432 ± 39 kPa to 423 ± 39 kPa, NS). e, Changes in skin hydration were evaluated in 24 subjects following application of XPL and petrolatum with post hoc analysis (Tukey method, $\alpha = 0.05$). XPL (116.65 μ S at 1 h) demonstrated significant increases in skin hydration compared with petrolatum (P) (42.65 μ S at 1h; p < 0.05), and untreated control sites (UC) (21.95 μ S at 1h; p < 0.001). The error bars represent the standard errors of the mean. Data sets marked with asterisks (*) represent statistically significant differences using a paired Student's t-test.

Study A examined mechanical reshaping of the lower lid region. Study A explored the feasibility of reshaping of the lower lid region over time following the application of the XPL and the subsequent progression of the crosslinking reaction in situ. In older individuals, there is often a protrusion of the fat pad underlying the skin in the lower lid area. In this study, a 5-point 0-4 photonumeric lower lid herniation scale was introduced to quantify the changes in the extent of fat pad herniation following XPL treatment. We reasoned that the protrusion of the fat pad underlying the skin in the lower lid area could potentially be corrected by a steady, compressive force imparted to the skin by the XPL. In our two-step topical delivery system, the compressive force results from the collapse of the polymer coil network during solvent loss, rather than by the chemical bond formation during hydrosilylation. Therefore, in the selection of the lead XPL studied here, the solvents and their concentrations in the formulations were optimally selected to provide sufficient compression-based shrinkage of the skin with minimal discomfort.

As seen in Fig. 1b, perceivable reshaping of the lower lid region for a subject with severe bags (severity grade of 4) occurs as the

XPL reaction proceeds. To study the crosslinking kinetics of the XPL after the two-step topical delivery system on skin, the relative storage modulus of the XPL was measured in vitro as a function of time, following the introduction of the platinum catalyst, also shown in Fig. 1b. The start of the first inflection region of the curve corresponds to the initiation of the crosslinking reaction, which is analogous to the exposure of the Step 1 formulation on skin to the Step 2 formulation comprising 200 ppm platinum catalyst. The steep increase in the normalized storage modulus over approximately 100 s provides an indication of how quickly the XPL is generated in situ. The final region of the S-shape curve represents a slower rate of change in the modulus as the reaction asymptotically approaches completion. The delay in the onset of crosslinking indicated at times t < 0 was the effect of the catalytic stabilizer introduced in the sample preparation protocol to allow for sufficient working time to conduct experimental measurement. At t = 0 s, the crosslinking reaction was initiated. The storage modulus approached 80% of the plateau value at t = 175 s and then levelled off, corresponding to the approach of reaction completion. The photos of the subject shown at baseline, 2 min after XPL application, and 3 h following NATURE MATERIALS DOI: 10.1038/NMAT4635 ARTICLES

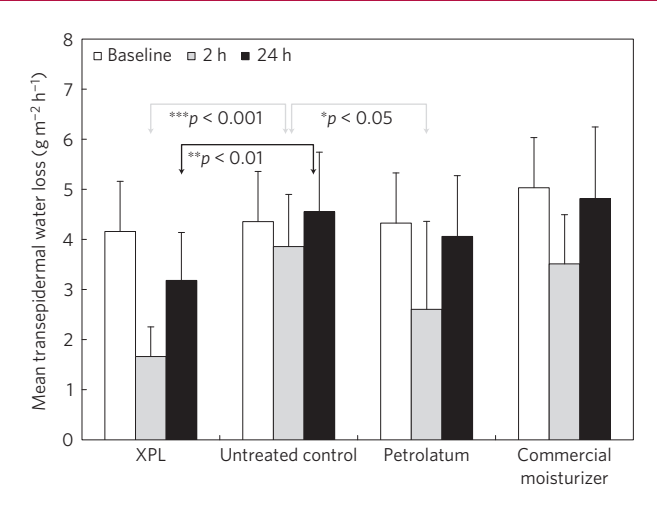


Figure 5 | Clinical data showing enhanced skin barrier function and sustained skin hydration for subjects (n = 22) with dry skin (Study C). At two hours, the sites treated with petrolatum and XPL demonstrated significantly reduced TEWL values compared with the untreated control values (*p < 0.05 and **p < 0.001). A reduction in the TEWL was sustained with the XPL over the course of 24 h (***p < 0.01). At 24 h, the differences measured for P and for commercial moisturizer were not statistically significant when compared to the UC. The error bars represent one standard deviation from the mean. The p values were calculated on the basis of one-way ANOVA analyses.

XPL application depict the immediate impact of the XPL on flaccid skin, followed by the impact on bag compression that occurs over a longer time frame (3 h to peak). This immediate effect reflects the rapid XPL crosslinking kinetics depicted in Fig. 1b, where close to 80% of the final elastic modulus value was achieved over the course of 2 min. Notably, the fat pad herniation demonstrated a 2-grade improvement, shown additionally in Fig. 2. Such a result has been previously achieved only by a lower lid blepharoplasty, an invasive surgical procedure. Sequential frames extracted from a time-lapse video (Fig. 3) demonstrated recovery of skin elasticity after XPL application to lax skin (Fig. 3a). The skin was tented (pinched) for 3 s with equal pressure on the XPL-treated (right) and XPL-untreated (left) lower lids and then released (Fig. 3b). Immediately after the skin was released (Fig. 3c), and 3 s (Fig. 3d) following release, there was a clear difference in the skin recoil between both sides. Whereas the right lower lid (XPL applied) retracted to its original shape, the untreated lid remained tented as a result of the remaining plastic strain from the imposed stress.

Study B examined improved elastic recoil of volar forearm skin. Study B explored the mechanical impact of the XPL layer on skin over a 24-h wear period and after XPL removal, to evaluate the XPL-induced modulation of skin elasticity during wear and the potential residual effects on the underlying internal skin stresses following XPL removal. The clinical changes in skin mechanical properties for six subjects were evaluated at baseline, following 24 h of XPL wear, and 35 min following XPL removal. Using a suction cup device, the volar arm skin was distended to a fixed position of 12% strain and then released. This test procedure enables the measurement of bulk skin retraction properties, a clinical indicator of skin mechanical function akin to the dermatologic skin tenting test. The negative pressure detected in the suction chamber scales with the skin distensibility, and the retraction times provide an indication of skin elasticity^{27,28}. Figure 4a shows a representative skin distensibility plot over five consecutive cycles of vacuum application to a representative untreated skin site at baseline. For the first cycle, the elastic and the viscoelastic regions are highlighted by the solid blue and red lines, respectively. As expected, under low strains,

the skin demonstrates linear elastic behaviour, corresponding to the initial linear increase in negative pressure with time; at higher strain, the skin exhibits viscoelastic behaviour with a corresponding nonlinear negative pressure dependence on time²⁹. Skin hysteresis was also observed over the five strain cycles, as characterized by the successive decrease in negative pressure required to induce the fixed strain (Fig. 4a).

The skin retraction properties corresponding to XPL-treated skin sites following 24 h of wear demonstrated a consistent, linear response (Fig. 4b). Compared with the untreated skin sites at baseline, the consistent linear slope resulting from sequential strain cycles with minimal hysteresis demonstrates the linear elastic behaviour exhibited by the bulk skin when the XPL is worn. With the XPL, faster retraction times were also measured along with lower negative pressures required to achieve the target distension height. Thirty-five minutes following XPL removal, the skin distension curve (filled diamonds) approached the baseline value, while not fully exhibiting the baseline viscoelastic behaviour, suggesting a transient skin memory resulting from the prior 24 h of XPL wear. In summary, the XPL-coated skin exhibited greater elasticity than normal, uncoated skin.

For the six subjects, significant decreases in the average skin retraction time and the average vacuum pressure corresponding to the 12% strain were also measured (36% and 28%, respectively in Fig. 4c,d), compared with the corresponding baseline values (Fig. 4b). Both measurements returned to the baseline values at 35 min following XPL removal.

Skin hydration resulting from XPL wear was evaluated in 24 volunteers, aged 22–55, using a skin surface hygrometer to measure skin conductance. The change in skin conductance from baseline values was calculated for sites treated with the XPL and with the petrolatum at baseline, 1, 2, 4 and 6 h following test article application (see Fig. 4e). Significant increases in skin conductance were measured for the petrolatum- and the XPL-treated sites (p < 0.05 and p < 0.001, respectively). Moreover, the XPL-treated sites demonstrated significantly higher increases in conductivity over the six hours of test article wear compared with the petrolatum-treated sites (p < 0.05). The skin hydration properties of the XPL were further complemented by the measurement of TEWL in subjects with clinically dry skin, described below.

Study C examined improved TEWL for dry skin. Study C explored the XPL aspect as a 'second skin' barrier against TEWL. The XPL barrier effect was measured on the legs of 22 volunteers with moderately to severely dry skin at the test sites, based on a 9-point visual dryness scale. In this study, the XPL was compared with petrolatum, the most effective skin occlusive reported in the literature³⁰, and a cosmetically elegant, 'high end' commercial moisturizer. An untreated control site served as the fourth test site. TEWL values were measured at baseline, 2 h, and at 24 h following test article application (Fig. 5). Two hours following test article application, the petrolatum- and the XPL-treated skin sites showed significantly decreased TEWL values relative to the untreated control sites (p < 0.05 and p < 0.001, respectively), whereas the cosmetically elegant moisturizer did not. At 24 h following test article application, a 23% decrease in the TEWL values from the baseline $(-0.95 \pm 0.41 \text{ g m}^{-2} \text{ h}, p < 0.01)$ persisted at the XPL sites, whereas there was no decrease in TEWL compared to baseline at the other sites. The results confirmed the XPL as a 'second skin' barrier that protects the skin from excessive moisture loss to the environment.

Study D examined second skin performance with normal wear. Study D explored the clinical performance of the XPL during normal wear in reshaping the lower lid. Notably, the elastic and adhesive properties of the XPL detailed above are important, as

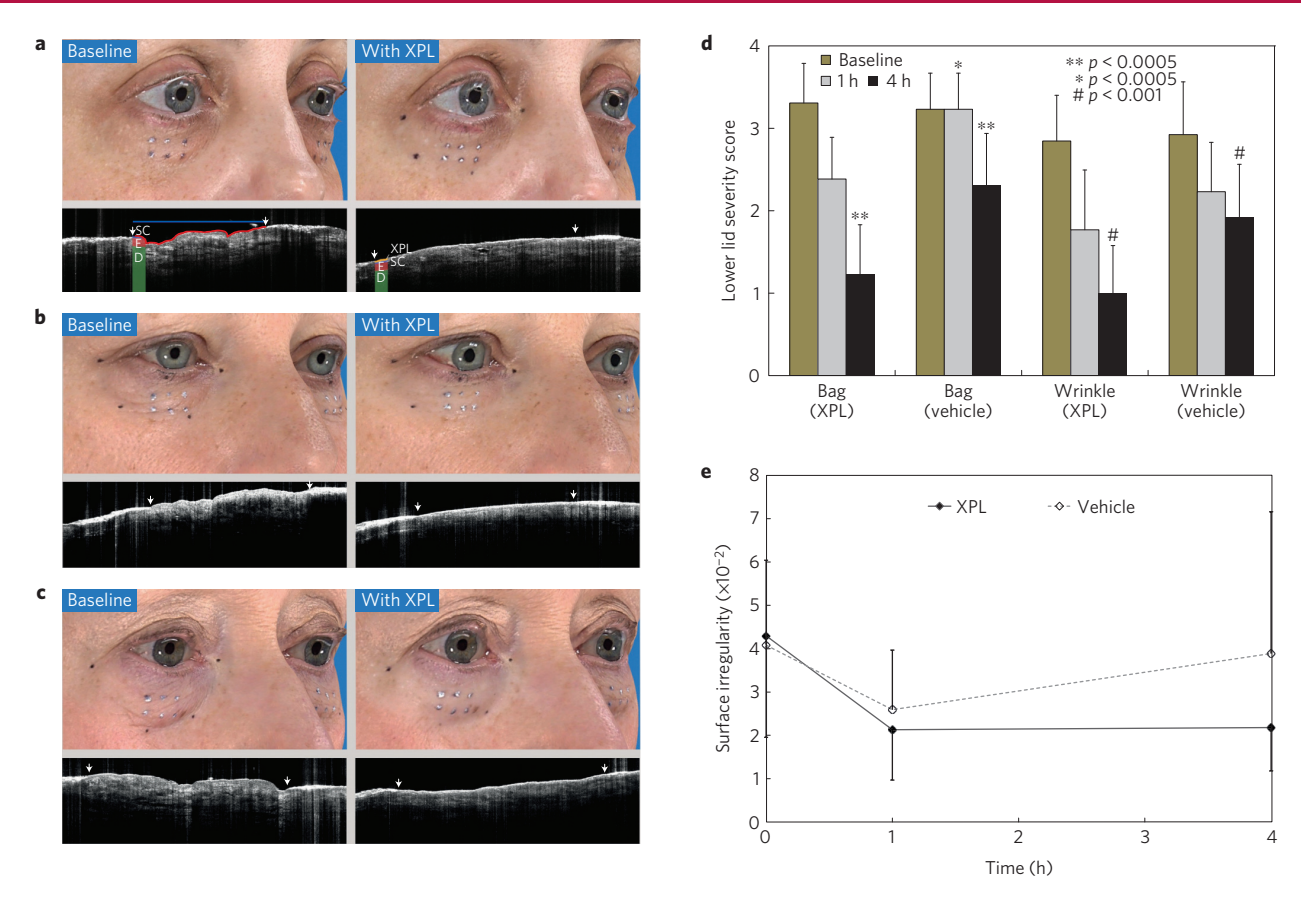


Figure 6 | Second skin performance with normal wear. a-c, Representative 3D photography (upper panels) and non-invasive imaging of the underlying epidermal layers using OCT (lower panels) for three subjects at baseline and 4 h after XPL application. The blue and red lines illustrate the two lengths used to calculate the surface irregularity. The three vertical pairs of metallic markers that were placed along the lower lid delineate the three different OCT measurement sites that were evaluated at each side. The two arrows in the OCT image correspond to the placement of one pair of markers. After 4 h, it is possible to visualize the XPL film over the stratum corneum. The stratum corneum (SC), epidermis (E), dermis (D) and XPL regions are identified in a. Pixel intensity analysis of the three OCT sections acquired at each application side at each time point for the twelve subjects suggested a greater level of hydration resulting from the XPL application compared with the vehicle at 4 h ($25,888\pm3,207$ versus $28,774\pm3,535$, respectively, p < 0.0001, paired Student's t-test), where lower pixel intensities represent a greater fraction of dark pixels, indicative of high water content. At baseline, the average pixel intensities measured were 31,477 ± 3,708 (XPL) and 30,878 ± 3,821 (vehicle), translating to decreases of 18% and 7% in the pixel intensities, respectively. d, Double-blind, randomized, placebo-controlled pilot clinical trial to evaluate XPL contractile function at the lower lid using 0-4 photonumeric scales for quantifying extent of skin response. At 1 h (2.38 ± 0.51) and at 4 h (1.23 ± 0.60) following test article application, the XPL demonstrated statistically significant (p < 0.0005) 1-grade and 2-grade improvements compared with the corresponding vehicle grades of 3.23 ± 0.44 and 2.31 ± 0.63 , respectively. The baseline average values for the XPL and the vehicle sites were 3.31 ± 0.48 and 3.23 ± 0.44 , respectively. The lower lid wrinkle values for the vehicle at baseline, 1h and 4h are 2.92 ± 0.64 , 2.23 ± 0.60 , and 1.92 ± 0.64 , respectively. For the XPL treatment sites, the wrinkle grades at the corresponding time points are 2.85 ± 0.55 , 1.77 ± 0.73 and 1.0 ± 0.58 , respectively. At four hours, a significant improvement in wrinkles was observed (p < 0.001) for the XPL side compared with the vehicle. The error bars represent one standard deviation of the mean. The symbols (*, **, #) identify data sets demonstrating statistical differences using a paired Student's t-test. e, The surface irregularity values measured from the triplicate OCT images obtained at each treatment side show significantly decreased skin surface roughness at four hours following XPL application compared with the vehicle control $(2.18 \times 10^{-2} \pm 1.00 \times 10^{-2})$ versus $3.89 \times 10^{-2} \pm 3.27 \times 10^{-2}$, respectively, p < 0.01). Zero surface irregularity values correspond to smooth surfaces with no measurable roughness. Baseline surface irregularity values showed no significant differences between the two groups $(4.30 \times 10^{-2} \pm 2.34 \times 10^{-2})$ versus $4.08 \times 10^{-2} \pm 1.96 \times 10^{-2}$, respectively), validating the randomization scheme used. At one hour, the difference measured between the two groups trended towards significance ($2.13 \times 10^{-2} \pm 1.16 \times 10^{-2}$ versus $2.59 \times 10^{-2} \pm 1.38 \times 10^{-2}$, respectively, p = 0.18). The error bars denote one standard deviation of the mean. The p values were calculated using paired Student's t-tests.

facial expressions invoke repeated stress and strain to the under-eye area, creating a challenge to the XPL 'second skin' durability during normal wear.

To begin characterizing the XPL-induced changes in skin mechanics and cosmesis, two 0–4 photonumeric scales were developed to enable quantification of XPL-induced skin shape changes by trained observers. The potential mechanisms responsible for the observed effects were further studied using optical coherence tomography (OCT) to non-invasively examine the underlying changes in the hydration and the mechanics of the skin that interfaces the XPL 'second skin'.

The placebo control (the vehicle-treated group) comprised a similar two-step formulation from which the catalyst was removed to prevent network crosslinking. The blinded and trained graders found significant improvements in bag severity at 1 and 4h after XPL application (Fig. 6d). The modest and statistically nonsignificant improvements from baseline in the vehicle-treated sites are likely to be due to the skin hydration properties of XPL and/or to the light scattering ingredients incorporated in the vehicle delivery of our two-step system. At one hour following test article application, both the XPL and the vehicle groups showed improvements in their average wrinkle severity grade, which did not

differentiate the effect of the XPL and the vehicle (not significant). At four hours, the continued improvement at the XPL-treated sites was observed to exceed the effects perceived at the vehicle-treated sites (p < 0.0001). Examples correlating the improvement of the lower lid following XPL application to the underlying changes in skin hydration are shown by pairing photographs with the corresponding OCT images (Fig. 6).

Over the course of four hours, the XPL-treated sites were significantly smoother than the vehicle control sites (Fig. 6e, 2.18×10^{-2} versus 3.89×10^{-2} , respectively, p < 0.01). The surface irregularity calculations also suggested a transient improvement in surface smoothness for the vehicle-treated sites compared with the baseline at 1 h (p < 0.001), which was likely to be an effect of hydration. By 4 h, however, the vehicle-treated site surface irregularity approached the corresponding baseline value, whereas the XPL-treated sites sustained their surface smoothness relative to baseline (p < 0.0001). This result is consistent with the visual assessment of a smoother skin surface with fewer irregularities at 4 h after XPL application, compared with the vehicle.

The OCT images were further analysed to quantify the change in pixel intensity resulting from the XPL and the vehicle treatments. Lucent pixels depict regions of low water content, whereas dark pixels indicate regions of increased hydration (Fig. 6). Within the viable epidermis, there was a significant decrease (p < 0.00001, see Supplementary Table 2) in the OCT pixel intensity during the 4 h following the XPL application compared with the baseline values (Fig. 6a–c), which we suggest was due to the enhanced skin barrier imposed by XPL wear, as suggested by the TEWL measurements. At 4 h, the average intensity for the XPL sections analysed was 10% lower than for the vehicle sections (p < 0.0001, see Supplementary Table 2), further supporting our interpretation that the XPL wear increases skin hydration.

In another study evaluating the XPL durability, 23 out of 25 subjects demonstrated excellent film integrity at the end of a 16-h wear period. Two of the 25 subjects showed a visible film boundary at the lower lid application site, although the XPL remained intact and adherent to the skin. Repeated daily wear resulted in no report of irritation or other adverse events resulting from the XPL use. Furthermore, the XPL remained intact following activities such as swimming, running and exposure to rain.

Discussion

We report here that a new, two-step, flowable polysiloxane-based formulation, applied topically and crosslinked *in situ* to form an 'invisible' thin film on human skin, can provide a durable, skin-conforming elastic 'second skin'. This 'second skin' is wearable, moisturizing, safe, well tolerated, and provides enhanced mechanical integrity to the underlying skin.

The XPL material design criteria for tensile modulus and elastic recoil were selected to mimic youthful skin properties, and the extent of elongation was selected to provide comfort through the range of motion the skin experiences. The material described here demonstrated a tensile modulus of 0.5 MPa, which was designed to cover the range of elastic response in normal healthy skin reported in the literature ^{24,25}. Such elastic recoil behaviour, and the 250% elastic strain region until fracture demonstrated by this material, are likely to be design parameters that promote the seamless integration of the XPL at the skin interface, thereby allowing for even extreme ranges of motion while providing the instantaneous recoil that is characteristic of youthful, intact skin.

The proof-of-concept human studies showed that XPL contraction reliably reshapes the skin surface, as well as mechanically flattening herniated fat pads that cause under-eye bagging. A double-blind, randomized, placebo-controlled study documented a marked decrease in under-eye bag severity and wrinkling that was significantly greater than that produced by the same composition without

the catalyst for crosslinking (vehicle-treated control), and hence, not attributable to the product moisturizing properties alone. A significant increase in the surface smoothness was also measured for the skin sites exposed to the XPL compared with the vehicle. Together, the double-blinded studies distinguish the contractile, mechanical effects achieved by the XPL crosslinked polysiloxane network on the cosmetic appearance of the skin from the vehicle effects that are likely to arise from skin hydration and optical manipulation of the skin surface. The visible flattening of the lower lid fat pad following 3 h of XPL application would also suggest that internal stress, or the XPL shrinkage, resulting from the volatiles loss is another important design parameter deserving additional characterization for effecting changes in skin shape.

The XPL also significantly decreased moisture loss from the skin, as evidenced by OCT imaging that quantified the increased state of epidermal hydration at sites exposed to the XPL. The OCT measurements were further supported by the quantitative measures of TEWL. Of note, the XPL performed better than a leading commercial moisturizer and a conventional highly occlusive agent, petrolatum, over the course of 24 h. Indeed, the elasticity and durability of XPL film on skin should also contribute to consistent barrier properties of the film, during wear. By comparison, the topical creams such as petrolatum or inelastic film formers such as Avalure UR 450 polyurethane exhibit plastic deformation that potentially may decrease the coating uniformity during wear. These localized variations in the film integrity may produce 'weak spots' that compromise barrier protection.

Overall, the observed elastic skin 'memory' is reasoned to result from the XPL-induced increases in skin hydration and/or the transient changes to the underlying skin tensile properties while interfacing the tangential XPL contractile stresses imposed at the skin surface. The potential of the XPL to impose a mechanical skin 'memory' that translates to a transient change in the underlying skin mechanical behaviour following removal of the XPL will be the subject of future studies examining the long-term benefits to skin following daily, repeated XPL wear. The association between anisotropic skin mechanical behaviour and the Langer lines is well documented in the literature²⁶. Skin anisotropy and the loss of skin mechanical integrity with age have been attributed to changes in the elastin and collagen architecture that constitute the dermis. The application of a thin, contractile layer to the stratum corneum leads to isotropic, tangential stresses exerted by the XPL in the plane of the skin. The role of these tangential stresses on modulating the anisotropic skin stress tensor deserves additional investigation. New devices that measure the in-plane stresses inherent to skin have further reinforced the anisotropic tension underlying skin mechanics³¹ and may be leveraged to characterize the in-plane mechanical changes induced by the XPL. Moreover, coupling these new techniques with additional detailed analyses of skin adhesion and the histology associated with the skin biomechanical responses utilizing human skin explant models may provide additional insight into the XPL-induced changes on the skin architecture. The elucidation of the mechanisms underlying the observed changes in the bulk skin mechanical behaviour resulting from the introduction of a thin skin-conforming layer at the surface, along with ongoing efforts to delineate the associated spatial changes in skin geometry, may offer additional insights into the material design criteria required for target indications addressed by the nextgeneration XPLs.

A wearable material layer that restores the normal skin mechanics and appearance is unprecedented and provides a platform to solve other cutaneous problems. Although the focus of this work has been to elucidate the impact of the elasto-mechanical properties of the XPL on skin, further directions of research and improvement to create better products for barrier protection and cosmetics present unique opportunities to enhance patient

compliance and quality of life. One such improvement might include extending the XPL wear beyond the current once-daily application specification. In addition, skin-adherent and skin-conforming polymers utilizing a similar concept could be developed as durable ultraviolet protection or as concealers of vascular anomalies such as port-wine stains. Devices that deliver pharmaceutical actives or assay biomarkers at the skin surface are additional potential applications. In summary, the XPL 'second skin' concept described here could potentially yield a next generation of functionalized second skins with broad medical benefits while allowing skin to look and behave naturally.

Methods

Methods and any associated references are available in the online version of the paper.

Received 15 May 2015; accepted 31 March 2016; published online 9 May 2016

References

- Irvine, A. D., McLean, W. H. & Leung, D. Y. Filaggrin mutations associated with skin and allergic diseases. N. Engl. J. Med. 365, 1315–1327 (2011).
- Schon, M. P., Boehncke, W. H. & Brocker, E. B. Psoriasis: clinical manifestations, pathogenesis and therapeutic perspectives. *Discov. Med.* 5, 253–258 (2005).
- Schon, M. P. & Boehncke, W. H. Psoriasis. N. Engl. J. Med. 352, 1899–1912 (2005).
- 4. Bieber, T. Atopic dermatitis. N. Engl. J. Med. 358, 1483-1494 (2008).
- Yosipovitch, G. & Bernhard, J. D. Clinical practice. Chronic pruritus. N. Engl. J. Med. 368, 1625–1634 (2013).
- Gilchrest, B. A. Skin aging and photoaging: an overview. J. Am. Acad. Dermatol. 21, 610–613 (1989).
- Balin, A. K. & Pratt, L. A. Physiological consequences of human skin aging. Cutis 43, 431–436 (1989).
- Anderson, R. R. Lasers for dermatology and skin biology. J. Invest. Dermatol. 133, E21–E23 (2013).
- Rushmer, R. F., Buettner, K. J., Short, J. M. & Odland, G. F. The skin. Science 154, 343–348 (1966).
- Kim, D. H., Xiao, J., Song, J., Huang, Y. & Rogers, J. A. Stretchable, curvilinear electronics based on inorganic materials. Adv. Mater. 22, 2108–2124 (2010).
- Rogers, J. A., Someya, T. & Huang, Y. Materials and mechanics for stretchable electronics. Science 327, 1603–1607 (2010).
- 12. Jang, K.-I. *et al*. Soft network composite materials with deterministic and bio-inspired designs. *Nature Commun.* **6**, 6566 (2015).
- 13. Mitragotri, S., Blankschtein, D. & Langer, R. Ultrasound-mediated transdermal protein delivery. *Science* **269**, 850–853 (1995).
- Kost, J., Mitragotri, S., Gabbay, R. A., Pishko, M. & Langer, R. Transdermal monitoring of glucose and other analytes using ultrasound. *Nature Med.* 6, 347–350 (2000).
- 15. Xu, S. *et al.* Soft microfluidic assemblies of sensors, circuits, and radios for the skin. *Science* **344**, 70–74 (2014).
- Clark, R. A., Ghosh, K. & Tonnesen, M. G. Tissue engineering for cutaneous wounds. J. Invest. Dermatol. 127, 1018–1029 (2007).
- Meddahi-Pellé, A. et al. Organ repair, hemostasis, and in-vivo bonding of medical devices by aqueous solutions of nanoparticles. Angew. Chem. Int. Ed. 53, 6369–6373 (2014).

- Davis, S. C. et al. The healing effect of over-the-counter (OTC) wound healing agents applied under semi-occlusive film dressing. Br. J. Dermatol. 172, 544–546 (2015).
- Borde, A. et al. Increased water transport in PDMS silicone films by addition of excipients. Acta Biomater. 8, 579–588 (2012).
- Hammock, M. L., Chortos, A., Tee, B. C., Tok, J. B. & Bao, Z. 25th anniversary article: the evolution of electronic skin (e-skin): a brief history, design considerations, and recent progress. *Adv. Mater.* 25, 5997–6038 (2013).
- Webb, R. C. et al. Ultrathin conformal devices for precise and continuous thermal characterization of human skin. Nature Mater. 12, 938–944 (2013).
- 22. Linear Polydimethylsiloxanes CAS No. 63148-62-9 (European Centre for Ecotoxicology and Toxicology of Chemicals, 2011).
- Lewis, L. N., Stein, J., Gao, Y., Colborn, R. E. & Hutchins, G. Platinum catalysts used in the silicones industry. Their synthesis and activity in hydrosilylation. *Platinum Met. Rev.* 41, 66–75 (1997).
- Annaidh, A. N., Bruyere, K., Destrade, M., Gilchrist, M. D. & Ottenio, M. Characterization of the anisotropic mechanical properties of excised human skin. J. Mech. Behav. Biomed. Mater. 5, 139–148 (2012).
- Agache, P. G., Monneur, C., Leveque, J. L. & Rigal, J. D. Mechanical properties and Young's modulus of human skin in vivo. Arch. Dermatol. Res. 269, 221–232 (1980).
- Hendriks, F. M. et al. A numerical-experimental method to characterize the non-linear mechanical behaviour of human skin. Skin Res. Technol. 9, 274–283 (2003)
- Manschot, J. F. & Brakkee, A. J. The measurement and modelling of the mechanical properties of human skin *in-vivo*–II. The model. *J. Biomech.* 19, 517–521 (1986).
- Diridollou, S. et al. In vivo model of the mechanical properties of the human skin under suction. Skin Res. Technol. 6. 214–221 (2000).
- Cua, A. B., Wilhelm, K. P. & Maibach, H. I. Elastic properties of human skin: relation to age, sex, and anatomical region. *Arch. Dermatol. Res.* 282, 283–288 (1990).
- 30. Kraft, J. N. & Lynde, C. W. Moisturizers: what they are and a practical approach to product selection. *Skin Ther. Lett.* **10**, 1–8 (2005).
- 31. Boyer, G. *et al.* Assessment of the in-plane biomechanical properties of human skin using a finite element model updating approach combined with an optical full-field measurement on a new tensile device. *J. Mech. Behav. Biomed. Mater.* **27**, 273–282 (2013).

Acknowledgements

The authors than \overline{L} G. Grove and Z. D. Draelos for their helpful discussions and M. Su for her assistance with the *in vivo* use studies.

Author contributions

B.Y., S.-Y.K., F.H.S., B.A.G. and R.R.A. contributed to the design and analysis of the *in vivo* use studies. A.A., N.R. and M.P. contributed to the design and development of material synthesis and topical formulation. A.A., N.R., M.P., A.N. and D.G.A. contributed to the characterization and analysis of the *in vitro* mechanical and rheological data. S.-Y.K. supervised the execution of the *in vivo* use studies. A.P. conducted *in vivo* Study B. B.Y. and R.L. managed the research efforts. B.Y., A.A., A.N., B.A.G., R.R.A. and R.L. wrote the manuscript with the help of the co-authors.

Additional information

Supplementary information is available in the online version of the paper. Reprints and permissions information is available online at www.nature.com/reprints. Correspondence and requests for materials should be addressed to R.L.

Competing financial interests

All of the authors hold a financial interest in Living Proof and/or Olivo Labs.

NATURE MATERIALS DOI: 10.1038/NMAT4635 ARTICLES

Methods

XPL two-step delivery system formulation development. To coat the skin with a thin and uniform layer of the lead RPB, formulation design efforts focused on the development of a new emulsion system comprising an aqueous-compatible internal phase and a siloxane-compatible external phase. The formulation development efforts required the incorporation of an internal phase thickener that enabled the appropriate shear-thinning effects to facilitate the deposition of the siloxane phase. When the siloxane phase was deposited too rapidly onto the skin, the uniformity of the XPL was compromised, yet a prolonged application 'playtime' interfered with the mechanical integrity of the crosslinked layer. Moreover, we constrained the total amount of non-volatile silicone-compatible ingredients that could act as plasticizers in the final XPL film to 2% (w/w) or less. Optimization of the formulation flow properties and the siloxane deposition time was achieved by adjusting the emulsifier and thickener chemistries, as well as the overall ingredient compositions, to provide a new delivery system that maintained the above RPB mechanical-adhesive attributes for the *in situ* crosslinked XPI film

After multiple rounds of formulation optimization, a two-step delivery system comprising the 'Step 1' and 'Step 2' formulations was developed. Water-in-silicone emulsion systems were developed to enable the delivery of the lead RPB (at 32% w/w) of Step 1 and the platinum catalyst (at 200 ppm w/w) of Step 2 through the continuous silicone phase. With this approach, Step 1 facilitated a consistent deposition of the lead RPB coating on skin that was subsequently crosslinked *in situ* to form the XPL film when exposed to the platinum catalyst in Step 2. The authors are not aware of other topical emulsion-based formulations that successfully incorporate such a high concentration of silica-reinforced polysiloxanes.

The Step 1 formulation containing the lead RPB demonstrated improved spreading properties on lax skin compared with the lead RPB alone. Plots of the instantaneous viscosity as a function of the shear rate illustrated a stronger shear-thinning effect of the Step 1 formulation containing the lead RPB, compared with the lead RPB alone, with a two- to threefold decrease in the instantaneous viscosity at shear rates above $5\,\rm s^{-1}$ (Supplementary Fig. 8). Note that maximum shear rates from 10^4 to $10^5\,\rm s^{-1}$ have been reported for the application of topical cream products on skin²8. The rheological behaviour of Step 1 allows the emulsion to exhibit lower viscosities at the high shear rates associated with topical formulation application, despite the comparable viscosities of 1,500 Pa s $^{-1}$ (Step 1 containing the lead RPB) and 1,800 Pa s $^{-1}$ (the lead RPB alone) measured at low shear rate of 0.15 s $^{-1}$. In addition, the high formulation viscosities measured at low shear rates support prolonged shelf-life stability by lowering the rates of gravity-driven sedimentation.

Finally, the XPL optical properties were adjusted to complement the light scattering properties of natural skin. The XPL optics were modulated by introducing light scattering particles into the Step 2 formulation such that these particles were deposited at the XPL surface. Surface-treated nylon particles with a particle diameter approximating 8 μm and a refractive index of 1.54 (Nylon 10-12, KOBO Products) provided the best optical match between the XPL and natural skin, following repeated clinical evaluation of several commercially available light scattering particles. Clinical examples of the optical effects are shown in Figs 1b, 2, 3 and 6.

Materials. Vinyl dimethicone, hydrogen dimethicone, and Karstedt platinum catalyst were purchased from AB Specialty Silicones. PMX-1184 (dimethicone and trisiloxane), FZ-2233 (bis-isobutyl PEG/PPG-10/7/dimethicone copolymer), and DC-9045 (decamethylcyclopentasiloxane and dimethicone crosspolymer) were purchased from Dow Corning Corporation. KSG-240 (dimethicone/PEG-10/15 crosspolymer and decamethylcyclopentasiloxane) and KF-995 (decamethylcyclopentasiloxane) were purchased from Shin-Etsu Chemical Corporation. Pemulen TR-2 (acrylates/C10-30 alkyl acrylate crosspolymer), Ultrez 20 (acrylates/C10-30 alkyl acrylate crosspolymer) and waterborne polyurethane dispersion Avalure UR 450 polymer (PPG-17/IPDI/DMPA copolymer) were purchased from Lubrizol Corporation. Jeecide CAP-4 (phenoxyethanol and caprylyl glycol) and Jeechem BUGL (butylene glycol) were purchased from JEEN International. Glycerin and propylene glycol were purchased from Ruger Chemical. Sodium chloride and sodium hydroxide (10N) were purchased from Spectrum Chemical MFG. Nylon 10-I2 (Nylon 12 and isopropyl titanium triisostearate) was purchased from Kobo Products.

The lead RPB emulsion or Step 1 comprised 32% RPB 6 (see Supplementary Table 1), 12% PMX-1184, 4% KSG-240, 0.1% FZ-2233, 50.32% water, 0.5% Pemulen TR-2, 0.5% Ultrez 20, 0.33% Jeecide CAP-4, and 0.25% 10 N sodium hydroxide solution.

The platinum catalyst delivery system or Step 2 comprised 10% DC9045, 4% KSG-240, 0.2% FZ-2233, 15.79% decamethylcyclopentasiloxane, 4.5% Nylon 10-12, 29.50% water, 0.5% sodium chloride, 0.5% Jeecide CAP-4, 20% propylene glycol, 10% butylene glycol, 4% glycerin and 1.01% Karstedt platinum catalyst solution (2% platinum). The polyurethane and silicone wound dressing sheets were purchased from 3M (Tegaderm Transparent Film Dressing 1626W) and

Smith & Nephew (Cica-Care Silicone Gel Sheet). The bi-phasic remover was provided by Living Proof.

Formulation procedures. *Lead RPB emulsion or Step 1.* In the main mixer, the lead RPB and emulsifiers were combined with the silicone phase diluents until a homogeneous mixture was visible. In a side mixer, the aqueous phase containing the polyacrylic acid hydrogel and preservatives were mixed until the aqueous dispersion was homogeneous. The aqueous phase was slowly introduced to the main mixer containing the silicone phase to form a white creamy emulsion. Finally, the emulsion was neutralized to target pH of 5.5 to 6.5.

Platinum catalyst delivery system or Step 2. In the main mixer, the polysiloxane phase components and emulsifiers were mixed until the mixture was uniform. In a secondary mixer, the aqueous phase containing glycols, water and preservatives were mixed until the phase was homogeneous. The aqueous phase was slowly introduced to the silicone phase dropwise to form a clear emulsion. Nylon 10-12 was slowly introduced to the main mixer and the emulsion was then homogenized. Finally, the platinum catalyst solution was added to the emulsion and mixed until it was uniformly dispersed.

Mechanical testing. Uniaxial tensile tests were performed with an Instron 3342 (Norwood) based on ASTM D5083 methods. Briefly, a premix of the cure specimen (tetravinyltetramethylcyclotetrasiloxane/Karstedt platinum catalyst solution/RPB or the RPB emulsion; in a ratio of 0.5:0.5:99.0; w/w/w) was transferred into a dog bone mould (flat sheet type 0.5' wide) and cured for 24 h. The cure specimen was then subjected to either 15 load–unload cycles at 15% tensile strain or 25 load–unload cycles at 100% tensile strain at room temperature to obtain a stress–strain plot or a hysteresis loop. Then, the cure specimen was subjected to a full tensile load until break where the tensile modulus and the fracture strain were evaluated from the stress–strain response.

Adhesion-in-peel tests were conducted using an Instron 3342 based on ASTM C794 methods. Briefly, 0.75 g of a cure specimen premix (tetravinyltetramethylcyclotetrasiloxane/Karstedt platinum catalyst solution/RPB or the RPB emulsion; in a ratio of 0.5:0.5:99.0; w/w/w) was sandwiched in between two leather strips with a contact surface area of 1 inch by 2.5 inches and cured for 24 h. The peel test procedure subjected one side of the cured leather strip to a $10~{\rm mm~s^{-1}}$ extension until the leather strips completely separated. The adhesive force was averaged over the entire length of the cured location and normalized to the width of the sample.

Rheometer tests developed for measuring the crosslinking kinetics were conducted using the Bohlin CVO Rheometer (Malvern) to implement a dynamic mechanical test based on ASTM D7750 standards. Briefly, a premix of the cure specimen (tetravinyltetramethylcyclotetrasiloxane/Karstedt platinum catalyst solution/RPB or the RPB emulsion; in a ratio of 0.67:0.33:99.0; w/w/w) was transferred to a 25-mm flat plate with a 250- μ m gap size on the rheometer. The experiment was conducted at 70 $^{\circ}$ C under the oscillatory mode with a 1-Hz frequency to obtain a plot of the storage modulus (G') over time.

Pilot human studies. Normal volar forearm skin recoil study (Study B). The study protocol was approved by the Allendale IRB. Briefly, 6 women, ages 40 and older, were enrolled in the study. Duplicate volar forearm skin sites of 3 cm by 3 cm in area per panelist were assigned to three different treatments, XPL, AmLactin Moisturizing Body Cream (Upsher Smith Laboratories), and an untreated control site, following a predetermined randomized scheme. Measurements were taken at baseline, 24 h after test article application and 35 min following test article removal. A 0.08 ml volume of the lead RPB emulsion (Step 1) and 0.12 ml of the platinum catalyst delivery system (Step 2) were applied to each designated site to create the XPL. AmLactin (0.05 ml) was applied twice daily to the corresponding sites. The remover (1.5 ml) was applied to each of the eight sites evaluated after the 24-h measurement and left in contact with the XPL for at least 30 s to saturate and swell the film. The swollen film was then rolled off the skin using a cotton pad. Residual test article was removed with a dry tissue.

All suction cup measurements were taken following a 25–30 min acclimation period in a controlled environment with the relative humidity maintained at less than 50% and temperature maintained at 19–22 °C. A DermaLab USB (Cortex Technology) with a suction cup was used to evaluate skin elasticity following methods described in the literature 32,33 . Statistical analyses were conducted using a paired Student's t-test.

Skin conductance was measured in 24 volunteers (aged 25 to 55 years old) using a skin surface hygrometer (USB Dermalab with a flat-faced hydration probe, Cortex Technology) for two test articles: petrolatum (Vaseline, Unilever) and XPL. To enable probe contact with the skin during XPL wear, an annulus approximating the probe tip dimensions $(1.4\,\mathrm{cm^2}$ area) was created at the centre of the 5 cm by 5 cm application site, where bare skin remained readily accessible to take the skin conductance measurements. All measurements were taken following a 25–30 min acclimation period in a controlled environment with the relative humidity

ARTICLES NATURE MATERIALS DOI: 10.1038/NMAT4635

maintained at less than 50% and temperature maintained at 19–22 $^{\circ}$ C. Measurements were taken at baseline and following test article application at 1 h, 2 h, 4 h and 6 h. Statistical analyses were conducted using Tukey's post hoc test.

Dry skin study evaluating TEWL (Study C). The study protocol was approved by the Allendale IRB. A 9-point dryness grading scale was used to characterize the extent of skin dryness, where a score of 0 refers to no dryness and a score of 8 refers to severe dryness with marked roughness. Healthy female volunteers, ages 40 and with visual dryness scores of 3, corresponding to moderately dry skin, or greater at each test site were included in the study.

Subjects were instructed to stop the use of all moisturizing products (soaps, lotions, sunscreens, insect repellents and so on) on their legs during a 3-day pre-conditioning period before testing. Shaving was allowed up to 3 days before the start of the study and after the completion of the 24-h measurements. Exercise or drinking of hot or caffeinated beverages within 2 h before each instrument visit was discouraged as this could affect the measurements. Intensive, heavy exercise promoting excessive sweating was not permitted. The subjects were also instructed to wear shorts or pants that could be rolled above the knees to each visit.

Exclusion criteria included women with a skin condition other than dry skin at the test sites (such as psoriasis, eczema and atopic dermatitis); subjects with marks (such as tattoos, and scars) at the test sites that might interfere with the visual grading, were also excluded from the study. Twenty-two subjects completed the entire study.

For each subject, two of the four test products were applied in duplicate to four of the five sites and the remaining site served as the non-treated control site. Test articles assigned to each site of the five outer calf test sites (three sites on one leg and two sites on the other leg) were based on a predetermined rotation scheme.

A total of 0.15 ml of each Step 1 and Step 2 formulation was applied to cover the entire application site. Approximately 0.05 ml of petrolatum (Vaseline, Unilever) and 0.05 ml of the commercial product (Crème De La Mer, Estee Lauder Companies) was applied to the corresponding designated test sites using a finger cot according to the randomization schedule. Expert graders were blinded to the application process.

Before baseline acclimation, subjects' test areas were cleansed with wet Kimwipes (Kimberly-Clark Corporation) and then patted dry with dry Kimwipes. The cleansing was as minimal as wiping twice with wet Kimwipes and subsequently 'patting dry' by stroking twice with dry Kimwipes. Five 5 cm by 5 cm skin test sites were then marked. Following the established methods described above, transepidermal water loss (TEWL) measurements were taken at baseline, two hours and twenty-four hours following test product application using a CyberDERM RG1 Evaporimeter (CyberDERM). Subjects reported for their 24-h visit and the investigator determined the film integrity of the XPL-treated sites. If the XPL was not minimally an 80% continuous film, the subject's participation in the study would end and day 2 measurements would not be taken. For the TEWL values, a one-way ANOVA was used to compare the net change from baseline at each time point. For all analyses, a two-tailed p < 0.05 was taken as the level of significance.

Double-blind, randomized, placebo-controlled, split-face evaluation of XPL performance (Study D). Optical coherence tomography (OCT, Michelson Vivosight OCT, Michelson Diagnostics) was used for non-invasive, *in vivo*, real-time skin microscopy imaging to elucidate the skin hydration and topical mechanical shaping mechanism of the XPL technology. The clinical study was reviewed and approved by the Western Institutional Review Board (WIRB protocol number 20121506). Subjects between the ages of 40–75 with baseline lower lid severity scores of 3 or 4, based on a 0–4 photonumeric lower lid severity scale, were the primary inclusion criteria. A score of 0 corresponded to the absence of lower lid fat herniation, as

visualized by the smooth facial contour observed from the lower lid to the cheek. A score of 4 described severe protrusion of the lower lid fat pad, where the lower lid fat pad extended beyond the midpoint of the distance defined by the lower lid to the cheek. For severe bags, the smooth facial contour is disrupted by the concavity of the boundary highlighting the bag. Twelve women were enrolled in the study.

Briefly, the XPL and a randomized placebo control were applied split face to the lower lid application sites following a predetermined randomization scheme. The placebo comprised the two steps of the XPL, or the vehicle, where the catalyst for the crosslinking reaction was absent from the platinum catalyst delivery system (Step 2). A Canfield Vectra 3D imaging system (Canfield Scientific) was used to capture the changes observed in the shape of the skin contours at baseline, 1 h, and 4 h following XPL application. OCT imaging and live trained grader evaluations were also conducted with the evaluator blinded to the treatments at the three time points.

Metallic skin markers were applied to the under-eye area of each subject to enable consistent placement of the OCT probe at the same skin sites for each time point. For each under-eye area, three sites were consistently imaged at each of the three time points. These markers are identified by the arrows in the corresponding OCT images (Fig. 6). These OCT images were analysed to quantitatively assess the skin surface shaping effect of the XPL, using ImageJ (National Institutes of Health).

The distance between the two epidermal markers was measured using a straight line (SLD). The epidermal surface length (ESL) was measured by tracing along the uneven epidermal surface in between the two markers. The surface irregularity values, described by the difference between the ESL and SLD (normalized by the ESL), were calculated at baseline, one hour, and four hours after XPL application. Values of surface irregularity that approach zero represent the ideal case of no surface roughness, as the ESL approaches the SLD.

The three sets of OCT image sections recorded for each skin site at baseline and at 4 h for the vehicle and for the XPL were further analysed to quantify the changes in the distribution of the pixel intensity. Sections of each image, comprising approximately 400 pixels in width and 40 pixels in thickness, immediately below the region identified as the stratum corneum, were selected by a blinded analyst. Owing to area constraints placed by the sample geometries for a limited number of images, the area analysed was reduced to remain contained within the epidermal layer. These image sections were then processed with ImageJ to calculate the average pixel intensity for each section selected. The ImageJ intensity scale is a 0–65,535 scale, corresponding to the dark and the lucent extremes of pixel intensity, respectively. After the average intensity was calculated for each site, the samples were un-blinded, and Student's *t*-test was implemented to determine the significance of the differences detected between the XPL and the vehicle groups.

Photography. Time-lapse photographs were taken using three digital single lens reflex cameras (two Nikon D80 and one Nikon D300), equipped with 17–70 mm macro lenses and circular polarizers, positioned to simultaneously photograph the subject at three angles: 45° angles from the left and the right, and one at the centre position. The subject was lit using three $1-\text{ft}^2-\text{LED}$ studio panel lights, each providing 1,400 LUX of 5,600 K lighting. Additional photographs were taken using a digital single lens reflex camera (Canon 5D Mark II) with an 85 mm lens (Sigma) and a strobe light unit (Alien Bees B800, Paul C. Buff) with an umbrella (Westcott) angled at approximately 45° towards the subject.

References

- Pedersen, L. & Jemec, G. B. Mechanical properties and barrier function of healthy human skin. Acta Derm. Venereol. 86, 308–311 (2006).
- Gniadecka, M. & Serup, J. in Handbook of Noninvasive Methods and the Skin (eds Serup, J. & Jemec, G. B. E.) 329–335 (CRC Press, 2006).